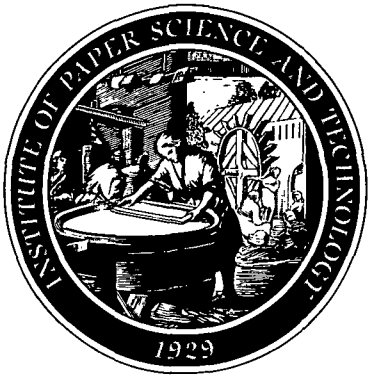

Institute of Paper Science and Technology
Atlanta, Georgia

IPST TECHNICAL PAPER SERIES

NUMBER 451

DETERMINATION OF CARBON MONOXIDE AND CARBON DIOXIDE CONCENTRATIONS AT TEMPERATURES BETWEEN 295-1250 K USING FOURIER TRANSFORM INFRARED ABSORPTION SPECTROSCOPY

P.J. MEDVECZ AND K.M. NICHOLS

JULY 1992

INTRODUCTION

FT-IR absorption spectroscopy is potentially an excellent technique for the *in situ* analysis of gas concentrations and temperatures in a high temperature combustion environment. Nearly all the species involved in combustion reactions are infrared active, with the exception of homonuclear diatomic molecules. The infrared beam is relatively unaffected by small particles and intense luminosity which often accompany combustion environments.[1] Finally, all species absorbing in the mid-infrared region are measured at the same time, making simultaneous multicomponent concentration determinations and temperature measurements possible.

Despite the advantages of FT-IR absorption spectroscopy, it has not been extensively used for the determination of gas concentrations at high temperatures (500-1250 K) in either a pure gas or a combustion environment. The technique is based upon a line-of-sight measurement, which limits it to those combustion environments which are well defined in terms of concentration and temperature profiles (i.e. one dimensional flames). Concentration measurements at elevated temperatures are complicated by a lack of fundamental line broadening and line strength data at elevated temperatures. Although there have recently been model predictions for the broadening of CO[2] and CO_2[3] at high temperatures, accurate experimental line strength data at high temperatures are not available. Finally, moderate resolution FT-IR instruments significantly distort the recorded peak heights due to the finite resolution of the instrument[4] making it difficult to accurately (quantitatively) interpret FT-IR spectra. This requires that peak heights recorded by the instrument be numerically corrected before they are used for gas concentration calculations.

Despite these complications, FT-IR absorption spectroscopy has been used previously in combustion environments. Ottesen and Thorne[1,5] used FT-IR for the determination of gas temperatures and CO and CO_2 gas concentrations in a coal combustion environment. They used the Bouguer-Lambert law to equate the absorption intensity of a single vibrational-rotational line to the product of the line

strength, partial pressure of the gas, and the path length. Line fitting infrared absorption spectra for the analysis of high temperature gases in combustion systems has been used much more extensively with other spectroscopic techniques. Hanson and coworkers[6,7] and others[8,9] have used tunable diode lasers to obtain absorption spectra of single vibrational-rotational lines. They then used line fitting techniques to calculate either line strengths,[6,8] collision linewidths,[6-9] or gas concentrations.[6-9] Although tunable diode lasers have a higher instrument resolution than FT-IR spectrometers, their small frequency range (~1 cm^{-1}) limits the technique to single species measurements.

Before FT-IR absorption spectroscopy is applied to a combustion environment for the determination of gas concentrations and temperatures it has been necessary to develop appropriate experimental and computational methodologies in a well controlled high temperature environment. In a previous article, the development of techniques for the determination of gas temperatures (295-1250 K) using the vibrational-rotational lines of the CO fundamental band were presented.[10] In the present work the determination of CO and CO_2 concentrations at temperatures up to 1250 K are discussed.

THEORY

The absorption of infrared radiation by a gas for a single vibrational-rotational absorption line is given by the Bouguer-Lambert expression,[8]

$$T(\nu) = e^{-\alpha(\nu)CL} . \qquad \text{Eq. 1}$$

This relationship, equates the transmittance, $T(\nu)$, of a single vibrational-rotational line with the absorption coefficient, α, the gas concentration, C, and the path length of the cell, L. For most FT-IR spectrometers, the relationship between transmittance, $T(\nu)$, and absorbance, $A(\nu)$, is given by Equation 2,[4]

$$A(\nu) = -\log T(\nu) . \qquad \text{Eq. 2}$$

Substitution of Equation 2 into Equation 1 yields,

$$A^t(\nu) = \frac{\alpha(\nu) \cdot C \cdot L}{\ln(10)} \quad . \qquad \text{Eq. 3}$$

The superscript, t, distinguishes the true absorbance, $A^t(\nu)$, from an apparent or experimental absorbance, $A^a(\nu)$, as described by Anderson and Griffiths.[4]

The mathematical expression for the absorption coefficient, $\alpha(\nu)$, is dependent upon the conditions of the experiment, most importantly the total pressure of the gas. This dependence is a result of the mechanism controlling the broadening of the vibrational-rotational line. Gross, Griffiths, and Sun have given a description of the appropriate profiles for various conditions.[11] At one atmosphere pressure, collision broadening determines the vibrational-rotational line profile and a Lorentzian line shape is applicable,

$$\alpha(\nu) = \frac{S(m) \cdot \gamma(m)}{\left[\pi \cdot ((\nu - \nu_o)^2 + \gamma(m)^2)\right]} \quad . \qquad \text{Eq. 4}$$

Here, S(m) is the line strength ($cm^{-2}\ atm^{-1}$), $\gamma(m)$ is the half-width of the line (cm^{-1}), ν is the frequency, and ν_o is the frequency of the line center. The index of the line is denoted by m, where m is equal to -J" for a P branch line and J"+1 for a R branch line. The line strength is dependent upon m and, therefore, is different for each line used in the concentration calculations. Substitution of the expression for the absorption coefficient given in Equation 4, into the absorption intensity relationship given in Equation 3 yields,

$$A^t(\nu) = \frac{\gamma(m) \cdot L \cdot S(m) \cdot C}{\left[\pi \cdot ((\nu - \nu_o)^2 + \gamma(m)^2) \cdot \ln(10)\right]} \quad . \qquad \text{Eq. 5}$$

Solving Equation 5 to determine the gas concentration (partial pressure) has been accomplished previously by two different methods. The first, used by Ottesen and Thorne,[1,5] involves a line fitting technique. These authors used Equation 5 to generate a calculated spectrum of the same vibrational-rotational absorption line which they obtained experimentally. Using a non-linear least squares approach, they then adjusted the value for the partial pressure of the gas in the calculated spectrum until a good fit between the calculated line shape and the experimental line was obtained. They performed some photometric error corrections by assuming that the distortion could be approximated by increasing the value of γ in Equation 5.

Because of the moderate resolution of the instrument used in this work, 0.25 cm^{-1}, peak height corrections are necessary.[4] A line fitting approach similar to Ottesen and Thorne's would require photometric error correction calculations for many points for each vibrational-rotational line in order to generate a true experimental line shape. Explicitly correcting for the experimental data points of a single vibrational-rotational line is a computationally intensive process. If more than one calculated value for the gas concentration is desired, it is necessary for this process to be repeated for each line.

The approach taken in this work is different, and is similar to Sell's.[8] This alternate approach involves solving Equation 5 for the peak center, ν_o,

$$A^t(\nu_o) = \frac{L \cdot S(m) \cdot C}{\left[\pi \cdot \gamma(m) \cdot \ln(10)\right]} \quad . \qquad \text{Eq. 6}$$

The concentration of the gas is then obtained by correcting only the peak center apparent absorbance and using this value in Equation 6 to directly calculate for the gas concentration. By making peak height corrections for the peak maxima of several vibrational-rotational lines, multiple independent measurements of the gas concentration can be obtained. These values can then be used to obtain an average gas concentration.

Three factors which most strongly influence the relative intensity of vibrational-rotational absorption lines are the absorption coefficient, $\alpha(m)$, the concentration of the gas, and the path length. Each of these is directly proportional to the absorption intensity, as described by Equation 6. While the influence of concentration and path length on absorption intensity is intuitive, the factors comprising the absorption coefficient are less obvious and more complicated. The two variables comprising the absorption coefficient are the line half-widths and the line strengths. Line strengths are strongly dependent upon the gas temperature and m. Half-widths are not only m and temperature dependent, but are also dependent upon the partial pressure of all the components in the gas phase. Explicitly accounting for both the line strength and half-widths is necessary to performing high temperature concentration calculations.

High Temperature CO and CO_2 Half-Width Data

For gases at atmospheric pressure, collision broadening controls the line shape.[11] With this mechanism of line broadening, each species in the gas sample influences the width of the line. In addition, the half-width is dependent upon the value of m and the gas temperature. Equations have been developed to describe the half-width of absorption lines, $\gamma_x(m)$, in gas mixtures based upon the partial pressure of the gaseous components, P_x, P_y, etc.; the total pressure, P_T; broadening coefficients, $\gamma^\circ_{x,x}(m)$, $\gamma^\circ_{x,y}(m)$, etc.; the gas temperature, T; a reference temperature, T°; and the temperature exponents, $N_{x,x}(m)$, $N_{x,y}(m)$, etc.[11] For example, broadening for a two-component system consisting of species x and y is given by,

$$\gamma_x(m) = \gamma^\circ_{x,x}(m) \cdot \frac{P_x}{P_T} \cdot \left(\frac{T_o}{T}\right)^{N_{x,x}(m)} + \gamma^\circ_{x,y}(m) \cdot \frac{P_y}{P_T} \cdot \left(\frac{T_o}{T}\right)^{N_{x,y}(m)} . \qquad \text{Eq. 7}$$

Details describing this equation and the theories used to derive it are presented in greater detail by Gross *et al.*[11] Equation 7 provides the calculation methodology for line half-widths, however, its use requires either experimental, theoretical, or predicted (based upon a combination of theory and experiments) temperature and m dependent values of $\gamma^\circ_{x,x}(m)$, $\gamma^\circ_{x,y}(m)$, $N_{x,x}(m)$, and $N_{x,y}(m)$. The most

comprehensive and reliable source for this data has been found from modeling work performed by Hartmann *et al.*[2] for CO lines and by Rosenmann *et al.*[3] for CO_2 lines.

Hartmann *et al.*[2] developed a model which accounts for CO line broadening by H_2O, N_2, O_2, and CO_2. This model is based, in part, on existing high temperature experimental broadening data and upon theoretical considerations. Their calculations have yielded values of γ° and N, including their dependence on m and temperature. This appears to be the most comprehensive data base available from which high temperature CO half-width information can be obtained. Values of CO self-broadening coefficients have been reported by Nakazawa and Tanaka[12] and by Anderson and Griffiths[13]. When these data must be used, the temperature exponent is assumed to be a constant, independent of both the broadening species and m value. The value of 0.75 is used for the temperature exponent, as described by Gross *et al.*[11]

Similarly, Rosenmann *et al.*[3] developed a model which accounts for CO_2 line broadening by CO_2, H_2O, N_2 and O_2 in the temperature range of 300-2400 K. Like the CO model, this model is again based upon both experimental broadening data and theoretical considerations. The model predicts values of γ° and N, including their dependence on m and temperature which can be used in Equation 7 for CO_2 half-width calculations. This model has been used in this work for both CO_2 self broadening and N_2 broadening of CO_2 lines.

Temperature Dependence of Line Strengths

There is very little experimental data which accurately describes the temperature dependence of the P branch CO lines or the R branch CO_2 lines used in this work. Because these values are not already available, it has been necessary to first experimentally determine the temperature dependence of CO and CO_2 line strengths at temperatures up to 1250 K. The calculation of line strengths is made by solving Equation 6 for, S(m), instead of gas concentrations. The revised equation is

for the CO_2 lines used in this work. Therefore, additional steps are required for these lines. These additional steps involve first correcting the experimental peak maxima for the overlap from neighboring lines, before using the values in calculations to determine the peak heights corrected for the finite resolution of the spectrometer.

For the first iteration, the peak heights are performed in a manner identical to those for the CO lines. These calculations result in approximate values of the true peak heights, A^t_{peak}. At the start of the second iteration the original experimentally obtained CO_2 peak heights, designated as A^a_{peak}, are corrected for the overlap from the two neighboring lines, resulting in a corrected peak, designated as A'^a_{peak}. These calculations are based upon the following set of equations, which are given below by example for line m=65,

$$A'^a_{peak}(65) = A^a_{peak}(65) - A^a_x(63) - A^a_z(67), \qquad \text{Eq. 9}$$

where x is the distance between the peak maxima of the m= 63 and 65 lines (which are the neighboring lines) and z is the distance between the m= 65 and 67 lines. This equation equates the overlap corrected experimental peak height with the original experimental peak minus the contribution of the lines on each side of it. The contributions from the neighboring lines is given by,

$$A^a_x(63) = -\log\left[\int_0^\infty \frac{\sin^2(\pi\cdot R_i\cdot(y\text{-}x))}{(\pi\cdot R_i\cdot(y\text{-}x))^2}\cdot\exp\left(\frac{-\ln 10\cdot A^t_{peak}(63)\cdot\gamma^2}{(x^2+\gamma^2)}\right)dy \Big/ \int_0^\infty \frac{\sin^2(\pi\cdot R_i\cdot(y\text{-}x))}{(\pi\cdot R_i\cdot(y\text{-}x))^2}dy\right] \qquad \text{Eq. 10}$$

$$A^a_z(67) = -\log\left[\int_0^\infty \frac{\sin^2(\pi\cdot R_i\cdot(y\text{-}z))}{(\pi\cdot R_i\cdot(y\text{-}z))^2}\cdot\exp\left(\frac{-\ln 10\cdot A^t_{peak}(67)\cdot\gamma^2}{(z^2+\gamma^2)}\right)dy \Big/ \int_0^\infty \frac{\sin^2(\pi\cdot R_i\cdot(y\text{-}z))}{(\pi\cdot R_i\cdot(y\text{-}z))^2}dy\right] \qquad \text{Eq. 11}$$

where R is the resolution of the instrument, and γ is the line half-width at half height. These equations are similar to those presented earlier,[10] except that they are solved at a point different than the peak maximum. Resulting from this series of integrations is a new set of "experimental" or apparent peak maxima. These new values for CO_2 peak heights are then used in the calculations, described previ-

ously, for the determination of true peak heights (corrected for the finite resolution of the spectrometer). With each successive iteration the corrected peak heights, A'^{a}_{peak}, improve as the values of the true peak height A^{t}_{peak} improve.

EXPERIMENTAL

Gas Cell and Optics

The gas cell and optics used for these experiments have been previously described.[10,15] Briefly, the cylindrical cell (inside diameter 3 7/8", inside length 3 3/4") was constructed of stainless steel and had 1" diameter sapphire windows on each end (General Ruby and Sapphire Co.). Inlet and outlet stainless steel tubes were put into the cell to allow a continuous stream of gas to flow through the cell. The inlet tube included a coil, 72" long, wound on the inside of the gas cell to preheat the gas to the cell temperature. A flow of gas continuously exited the cell through the outlet tube. The cell was heated by placing it inside an electric tube furnace (American Test Systems Model 3110) which was controlled by an LFE time proportioned temperature controller. The internal absolute pressure of the cell was continuously monitored using a pressure transducer (Omega Engineering, Inc., Model PX425) located on the gas outlet tube.

Because of the high temperatures of the furnace, the gas cell and furnace were located a short distance away from the interferometer. The infrared beam was brought to the gas cell through a series of mirrors (Optibus Components from Laser Precision Analytical). After passing through the gas cell the infrared beam was recollected and focused onto a wideband 0.25 mm mercury-cadmium-telluride (MCT) detector.

Specific precautions were taken to prevent stray radiation from the hot gas cell from becoming modulated and reaching the detector. Furthermore, procedures were developed to determine the instrument resolution, which is required for peak height correction calculations.[10,15]

Gas Samples

All the gas samples consisted of mixtures of CO, CO_2 and N_2. A total volumetric flow rate of 1 L/min was continuously passed through the cell. The gases used consisted of research grade CO and CO_2 (minimum purities of 99.997% and 99.998%, respectively) and prepurified N_2 (minimum purity 99.998%). The volumetric flow of individual CO, CO_2, and N_2 streams were measured either by mass flow meters (Teledyne, Hastings-Raydist, Model NALL-1,10 K) or rotameters (Brooks model 1355-V). Corrections to the mass flow meter readings were made for temperature, pressure, and gas species. No corrections were required for the rotameters which were operated at the same conditions as their calibration. The accuracy of all the meters was validated by comparisons with dry gas test meters. After being measured, the gases were combined and mixed in the tubing between their respective metering devices and the gas cell. After exiting the gas cell, the gas composition was rechecked using an NDIR CO/CO_2 gas analyzer.

Good agreement between the meter gas concentrations and the NDIR instrument were obtained from gas samples at room temperature. At higher temperatures, however, the agreement between metered concentrations and NDIR analyzer measurements was very poor. It was subsequently realized, that some of the CO put into the cell could undergo oxidative reactions with the cell wall or CO conversion to CO_2 and graphite by an equilibration reaction; thereby, changing the inputted gas composition. Therefore, only the NDIR measurements were used to determine the gas concentrations for samples at temperatures greater than room temperature.[15]

Data Collection

The absorption spectra recorded were all collected with a Laser Precision Analytical model RFX-75, FT-IR spectrometer, operating at a nominal instrument resolution of 0.25 cm^{-1}. Between 100-500 scans were coadded to obtain a single well resolved spectrum. Triangular apodization with 15-X zero filling was used to obtain the final spectrum. Triangular apodization was applied, since the convolution

of the line shape resulting from this apodization function and the Lorentzian line profile is easily numerically integrated. The high level of zero filling was used to improve the accuracy of the selection of peak maximum resulting from the experimental spectrum.

RESULTS AND DISCUSSION

A total of 123 spectra have been recorded in the high temperature gas cell to establish the accuracy of the calculation methodology. These spectra have been recorded at various temperatures ranging between 295 and 1250 K. For clarity in presenting and discussing the results, the spectra have been divided into three groups referred to as Data Set 1, Data Set 2, and Data Set 3.

Data Set 1 consists of 51 of the 123 spectra, which were used to determine the dependence of line strengths on temperature using the relation given in Equation 8. These spectra yielded 41 plots of line strength versus calculated temperature, one for each of the 41 CO and CO_2 absorption lines used. These plots are not included here but are reported elsewhere.[15] The line strengths determined from the spectra of Data Set 1 were used to calculate the CO and CO_2 concentrations from all 123 spectra, by using Equation 6 (solved for concentration).

Data Set 2 consists of 44 additional spectra, measured at the same furnace temperatures as Data Set 1. Data Set 2 verifies the accuracy of extending the line strength relationships and calculation methodology to additional spectra, beyond those used to determine line strengths.

Data Set 3 consists of 28 spectra at furnace temperatures differing from and intermediate to the temperature levels of Sets 1 and 2. Data Set 3 verifies the accuracy of using the technique at temperatures which are not the same as those used for determining line strengths. Though none of the raw spectral data are shown here, these have been reported[15] and are of the same high quality as those spectra presented previously for temperature determinations.[10]

Concentration Results From Data Set 1

The results of the Set I concentration calculations are presented in Tables 1 and 2. Each of these tables first includes general data regarding the spectra, including; the furnace set point temperature, the number of spectra recorded at that temperature, the range of concentrations which were measured at that temperature, and the average calculated temperature. Comparisons of the calculated (from FT-IR spectra) concentrations to the measured (by NDIR) concentrations are given in the three columns that follow. In the first of these columns is presented the average absolute percent concentration difference. The calculation of the percent difference is defined by,

$$\% \text{ Difference CO Concentration} = \frac{100 \cdot (\text{Measured CO} - \text{Calculated CO})}{\text{Measured CO}}. \qquad \text{Eq. 13}$$

The average absolute percent difference is the numerical average of the absolute percent difference calculated for each spectrum at a given furnace temperature. The next two columns contain the low and high calculated percent differences from each group of spectra at a given furnace temperature. In all cases, gas temperatures reported in these tables have been calculated from CO absorption spectra.

Because the gas concentration is measured from each absorption line, the concentration determined from one spectrum is really an average of the calculated concentrations from each line in that spectrum. The variability among the lines comprising the average was calculated as a standard deviation in units of percentage (% concentration). The average standard deviation, reported in the final column, is calculated by averaging the standard deviations from each of the spectra at a given furnace temperature.

The deviations between measured and calculated concentrations for the spectra of Data Set 1, are small. The average absolute percent differences for both CO and CO_2, ranged between 1.3 and 4.8% at all temperatures, except for the CO_2 1273 K spectra which had an average value of 8.8%. The overall percent differences are 3.2% and 4.6% for CO and CO_2, respectively. The low and high values

comprising each set were negative and positive respectively, for most temperatures, indicating that the data were not biased on either side of zero. Among the individual spectra, the variability ranged from a worse case low value of -15.97% (also for the CO_2 1273 K spectra) to the worse case high value of 11.67%.

The standard deviation for the variability among the lines at each furnace temperature ranged between 0.03-0.10%. To provide additional details regarding these values, the individual standard deviations of the six 773 K spectra (representing the 4th row in Table 1) are presented in Table 3. These results indicate that the variability of the calculated concentrations, among the lines, is relatively low, less than 5%. This suggests that there is good agreement among the lines, regarding the actual gas concentration of the sample. The variations shown for these values are typical of those found for the other temperatures.

Concentration Results from Data Set 2

Results for the CO and CO_2 concentration calculations from the 44 spectra of Data Set 2 are presented in Tables 4 and 5. These spectra were recorded under the same conditions, and at the same furnace set point temperatures, as those in Data Set 1.

The average absolute percent differences ranged between 1.8-4.0% for the CO spectra and between 2.5-5.1% for the CO_2. Among the individual results the lowest percent difference, among both the CO and CO_2 data, was -9.6% and the highest was 13.9%. The calculations for the average standard deviations among the lines ranged between 0.04-0.18%. The low and high values for each furnace set point temperature were negative and positive, respectively, again indicating no bias among the calculated results.

The results obtained from this set are as good as those described in Set 1; the overall percent differences are 2.7 and 4.2% for CO and CO_2, respectively. There appears to be no bias in the calcula-

tion methodology with regard to the gas temperature. The similarity of these results with those of data Set 1 are additional evidence that the line strengths have been accurately measured.

Concentration Results from Data Set 3

The concentration methodology was evaluated by a third data set. In this set, 28 spectra were recorded at temperatures intermediate to those used for the line strength data. The results of these calculations are shown in Tables 6 and 7.

For these spectra, the average absolute concentration differences varied between 3.0-8.2% for the CO spectra and between 3.9-12.6% for the CO_2. The low and high values among all the spectra were, at the worse case, -16.9 and 14.3%, respectively. The calculations of the variability among lines yielded average standard deviations which were between 0.04 and 0.17%. The overall average percent deviations for both the CO and CO_2 results are 5.2 and 6.3%, respectively.

The average absolute percent differences presented from this set are slightly higher then those presented in Sets 1 and 2. The data from Set 3 show a slight bias towards under predicting the gas concentrations. This is most evident for the CO_2 338 K spectra. It is likely that this error is a result of the inabilities of the line strength correlation to adequately account for the influence of peak overlap. This is consistent with the fact that the lines with lower m values are most strongly influenced by overlap and that at low temperatures fewer high m valued lines are available to offset this effect.

Despite this slight increase in the calculated percent differences, the results presented from this data set are still very encouraging. These data reveal that the calculation methodology is capable of accurately predicting gas concentrations at temperatures different than those where the line strengths have been measured.

CONCLUSIONS

The data presented illustrate the potential of FT-IR absorption spectroscopy for the determination of gas concentrations in a high temperature environment. The overall accuracy is between 3-7%, for spectra at temperatures between 295-1250 K and at CO and or CO_2 concentrations between 0.5-5% percent.

The success of these results is a product of the rigor used in the many preliminary steps; most importantly, the correction of peak heights for both the finite resolution of the spectrometer and peak overlap. The combined ability to determine the gas temperature and concentration from absorption spectra recorded in the heated gas cell of this study, provides the methodology to make similar measurements in a combustion environment.

ACKNOWLEDGMENTS

The authors gratefully acknowledge the financial support obtained from the U.S. Department of Energy under grant DE-ACO2-83CE40637 and also that obtained from the Institute of Paper Science and Technology and its member companies. We also acknowledge the generous technical support offered by the personnel of Laser Precision Analytical. In addition, the authors wish to thank Professor James A. de Haseth of the University of Georgia, Athens, for his expert advice.

Portions of this work were used by Patrick J. Medvecz as partial fulfillment of the requirements for the Ph.D. degree at the Institute of Paper Science and Technology.

1. L. R. Thorne, and D. K. Ottesen, Proc. - Electrochem. Soc. **83-7**, 425 (1983).

2. J. M. Hartmann, L. Rosenmann, M. Y. Perrin, and J. Taine, Appl. Opt. **27**, 3063 (1988).

3. L. Rosenmann, J. M. Hartmann, M. Y. Perrin, and J. Taine, Appl. Opt. **27**, 3902 (1988).

4. R. J. Anderson, and P. R. Griffiths, Anal. Chem. **47**, 2339 (1975).

5. D. K. Ottesen, and L. R. Thorne, Proc. - Int. Conf. Coal Sci., 351 (1985).

6. R. K. Hanson, Proc. SPIE-Int. Soc. Opt. Eng. **438**, 75 (1983).

7. P. L. Varghese and R. K. Hanson, J. Quant. Spectrosc. Radiat. Transfer **26**, 339 (1981).

8. J. A. Sell, J. Quant. Spectrosc. Radiat. Transfer **23**, 595 (1980).

9. H. S. Lowry, III and C. J. Fisher, J. Quant. Spectrosc. Radiat. Transfer **31**, 575 (1984).

10. P. J. Medvecz, K. M. Nichols, D. T. Clay, and R. Atalla, Appl. Spectrosc. **45**, 1350 (1991).

11. L. A. Gross, P. R. Griffiths, and J. N.-P. Sun, "Temperature Measurement by Infrared Spectrometry", in Infrared Methods for Gaseous Measurements, J. Wormhoudt, Ed. (Marcel Dekker, Inc., New York, New York, 1985), Chap. 3.

12. T. Nakazawa and M. Tanaka, J. Quant. Spectrosc. Radiat. Transfer **28**, 409 (1982).

13. R. J. Anderson and P. R. Griffiths, J. Quant. Spectrosc. Radiat. Transfer **17**, 393 (1977).

14. L. S. Rothman, Appl. Opt. **20**, 791 (1980).

15. P. J. Medvecz, "Spectroscopic Evaluation of the Gas Phase Above a Burning Black Liquor Char Bed", Ph.D. Dissertation, Atlanta, Georgia, The Institute of Paper Science and Technology, (1991).

Table 1. Data Set I: results of CO gas concentration calculations.

Furnace Set Point Temp. (K)	# of Spectra	Measured Conc. Range (%)	Calculated Avg. Gas Temp. (K)	Average Abs. % Diff of Calc.CO Conc.	Low (%)	High (%)	Variability Among Lines Avg. SD (%)
295	10	0.59-2.38	294	3.84	-7.2	6.8	0.04
373	6	0.78-2.94	353	3.30	-5.2	6.0	0.05
573	6	0.79-3.83	535	1.24	-2.5	3.1	0.06
773	6	0.60-4.06	720	2.93	-3.6	8.3	0.06
973	6	0.55-4.27	936	4.09	-4.9	10.9	0.03
1073	6	0.55-3.25	1034	1.32	-4.0	2.0	0.03
1173	6	0.58-3.94	1144	4.70	-10.1	7.6	0.04
1273	5	1.21-4.32	1227	3.86	-5.0	-4.32	0.08

Table 2. Data Set I: results of CO_2 gas concentration calculations.

Furnace Set Point Temp. (K)	# of Spectra	Measured Conc. Range (%)	Calculated Avg. Gas Temp. (K)	Average Abs. % Diff of Calc.CO_2 Conc.	Low (%)	High (%)	Variability Among Lines Avg. SD (%)
295	6	0.72-2.87	294	3.69	-10.45	3.90	0.03
373	6	0.85-2.78	353	3.30	-5.88	8.63	0.03
573	6	0.81-3.91	535	4.76	-7.41	10.23	0.10
773	6	1.01-4.20	720	4.73	-8.91	11.67	0.09
973	6	1.00-4.29	936	4.23	-7.14	7.69	0.07
1073	6	1.02-4.86	1034	2.85	-3.89	4.32	0.07
1173	6	1.29-4.77	1144	4.10	-5.03	5.45	0.10
1273	5	1.40-4.96	1227	8.80	-15.97	7.86	0.08

Table 3. Measured and calculated CO concentrations for the six spectra recorded at a furnace temperature of 773 K. Also included are the standard deviations and the relative percent standard deviations of the 41 lines which have been averaged to obtain the average concentration for each spectrum.

Measured CO Conc. (%)	Calculated CO Conc. (%)	Standard Deviation (%)	Relative Percent Standard Deviation
0.60	0.65	0.02	3.3%
1.51	1.52	0.07	4.6%
1.24	2.16	0.06	2.8%
2.90	2.81	0.06	2.1%
3.40	3.36	0.05	1.5%
4.06	4.03	0.13	3.2%

Table 4. Data Set 2: results of CO gas concentration calculations.

Furnace Set Point Temp. (K)	# of Spectra	Measured Conc. Range (%)	Calculated Avg. Gas Temp. (K)	Average Abs. % Diff of Calc.CO Conc.	Low (%)	High (%)	Variability Among Lines Avg. SD.
295	6	0.73-2.44	295	2.83	-3.74	5.48	0.06
373	6	0.96-2.91	352	2.11	-4.17	1.82	0.09
573	6	0.99-3.96	532	2.69	-5.05	5.05	0.08
773	6	0.87-4.58	723	1.80	-2.30	4.07	0.11
973	6	0.81-4.49	930	2.70	-4.82	-1.23	0.04
1073	6	0.78-4.20	1033	3.04	-5.63	0.00	0.04
1173	4	0.89-4.28	1130	2.83	-6.27	0.89	0.07
1273	4	2.31-4.49	1248	4.01	-5.54	-2.45	0.18

Table 5. Data Set 2: results of CO_2 gas concentration calculations.

Furnace Set Point Temp. (K)	# of Spectra	Measured Conc. Range (%)	Calculated Avg. Gas Temp. (K)	Average Abs. % Diff of Calc.CO_2 Conc.	Low (%)	High (%)	Variability Among Lines Avg. SD.
295	6	0.86-3.24	295	4.48	-9.65	0.37	0.04
373	6	1.05-3.06	352	5.13	-9.52	6.54	0.05
573	6	1.10-4.10	532	4.87	-4.55	13.90	0.16
773	6	1.12-4.58	723	5.05	-4.71	10.92	0.13
973	6	1.12-4.48	930	2.50	-1.17	7.37	0.07
1073	6	1.18-4.86	1033	3.70	-3.23	8.23	0.10
1173	4	1.21-4.53	1130	3.35	-7.10	1.77	0.08
1273	4	2.57-4.86	1248	4.24	0.78	8.85	0.13

Table 6. Data Set 3: results of CO gas concentration calculations.

Furnace Set Point Temp. (K)	# of Spectra	Measured Conc. Range (%)	Calculated Avg. Gas Temp. (K)	Average Abs. % Diff of Calc.CO Conc.	Low (%)	High (%)	Variability Among Lines Avg. SD.
338	4	0.99-2.68	330	7.72	-10.98	-4.08	0.06
473	4	0.99-3.83	441	4.22	-8.77	-1.31	0.09
673	4	0.58-3.61	634	8.16	-6.37	14.33	0.08
873	3	1.34-3.62	854	5.02	-2.22	11.66	0.11
1073	4	0.52-3.11	978	4.94	-1.92	10.51	0.04
1123	4	0.58-2.83	1081	3.43	-7.02	-0.10	0.04
1223	4	0.70-3.50	1213	3.03	-1.88	4.99	0.08

Table 7. Data Set 3: results of CO_2 gas concentration calculations.

Furnace Set Point Temp. (K)	# of Spectra	Measured Conc. Range (%)	Calculated Avg. Gas Temp. (K)	Average Abs. % Diff of Calc.CO_2 Conc.	Low (%)	High (%)	Variability Among Lines Avg. SD.
338	4	1.09-2.68	330	12.62	-16.89	-9.75	0.05
473	4	0.99-3.72	441	3.92	-6.17	-1.59	0.10
673	4	1.35-3.72	634	7.44	-11.35	-2.67	0.17
873	4	1.36-4.10	854	5.96	-8.97	7.05	0.12
1073	4	1.33-3.81	978	5.24	-8.03	2.76	0.06
1123	4	1.29-4.20	1081	4.34	-6.42	-2.09	0.07
1223	4	1.28-3.81	1213	4.60	-1.24	8.82	0.07